IN VITRO ANALYSIS OF TIME-DEPENDENT RED BLOOD CELL PHASE SEPARATION IN A COMPLEX MICROCHANNEL NETWORK

Alberto Mantegazza [*1], Francesco Clavica[1,2], and Dominik Obrist[1]

[1]*ARTORG Center for Biomedical Engineering Research, University of Bern, Bern, Switzerland*
[2]*Integrated Actuators Laboratory, École Polytechnique Fédérale de Lausanne, Neuchâtel, Switzerland*

Summary In this study we provided quantitative data on red blood cell (RBC) partitioning in 21 divergent bifurcations embedded in a complex *in vitro* network. In the majority of bifurcations the branch receiving a higher blood fraction received an even higher RBC fraction (*classical partitioning*). However, in some bifurcations the low-flow branch received a higher RBC flow fraction (*reverse partitioning*). Moreover, we found that the phase separation is strongly time-dependent and some selected bifurcations oscillated between the two types of partitioning.

INTRODUCTION

The topology of microvascular networks is complex and characterized by multiple diverging and converging blood vessels and the red blood cell (RBC) partitioning (i.e. *phase separation*) at diverging bifurcations is non-uniform. In our recent study [1], the RBC phase separation was investigated in a microvascular network model featuring many sequential symmetric bifurcations (Figure 1(a)). The time-averaged results (Figure 1(b)) confirmed that in most diverging bifurcations the branch with the higher blood flow fraction Φ received an even higher RBC flux fraction Ψ (*classical partitioning*). However, in agreement with computational results [2], an inversion of the classical phase separation behaviour (*reverse partitioning*) was observed for diverging bifurcations with skewed hematocrit profiles in the parent vessel. The hematocrit profile skewness (inset of Figure 1(b)) and the reverse partitioning were enhanced for high flow velocities.

In this study, we examined in detail the origin of these time-averaged phase separation results by investigating how cell partitioning evolves in time at specific bifurcations in the network (time-dependent phase separation).

MATERIALS AND METHODS

The PDMS microdfluidic device was fabricated via soft-lithography and replica molding. It embedded a network with 49 hexagonal elements and 176 microchannels. All microchannels dimensions (width $W = 10\ \mu m$, height $H = 8\ \mu m$ and length $L = 85\ \mu m$, Figure 1(a)) were inspired by the typical length scales found *in vivo*.

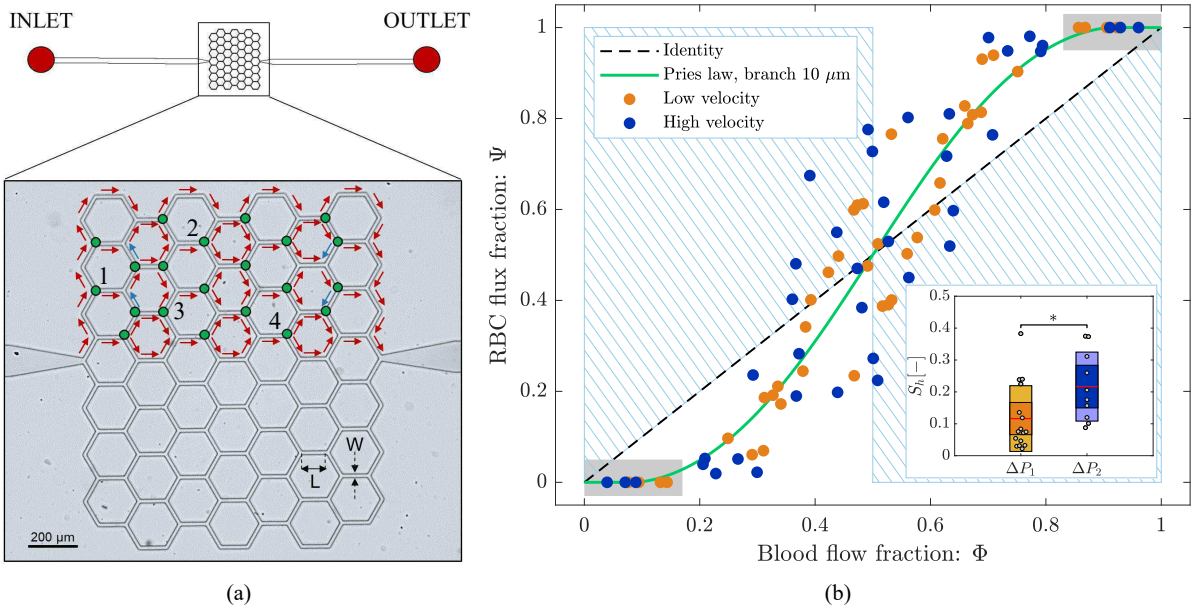

(a) (b)

Figure 1: (a) Microscope image of the microchannel network. Red and blue arrows indicate the direction of blood and plasma flow, respectively. Green dots represent diverging bifurcations considered in this study. (b) Phase separation results for the low (orange) and high (blue) velocity experiments (adapted from [1]). The green line is the empirical low from Pries [3]. The inset shows that the skewness hematocrit index (S_h) is statistically significantly ($p = 0.014$) higher for the high velocity experiment.

The working fluid was a suspension of RBCs at feeding hematocrit $H_f = 10\%$ dispersed in a water-based buffer fluid. The final solution matched the density and viscosity of physiological blood. The flow was controlled by setting a pressure

*Corresponding author. E-mail: alberto.mantegazza@artorg.unibe.ch.

difference between the fluid level in the reservoir and the device outlet ($\Delta P_1 = 35.3\ mbar$ and $\Delta P_1 = 47.1\ mbar$, hereafter referred as *low velocity* and *high velocity* experiments, respectively).

Particle Tracking Velocimetry (PTV) was performed on the image sequences to compute RBC velocity ($U_{rbc}[mm/s]$) and tube hematocrit ($H_t[-]$) in each channel of the top half of the network. Similarly to Mantegazza *et al.*[1], the RBC flux and the total blood flow rate in a Region Of Interest (ROI, $width = W_{ROI}$, $heigth = H_{ROI}$) were computed as

$$Q_{rbc}(t) = U_{rbc}(t) \times H_t(t) \times W_{ROI} \times H_{ROI}, \tag{1}$$

$$Q_{blood}(t) = U_{rbc}(t) \times W_{ROI} \times H_{ROI}. \tag{2}$$

The fractional RBC flux ($\Psi^i(t)$) and the fractional blood flow ($\Phi^i(t)$) in the daughter branch i were given by

$$\Psi^i(t) = \frac{Q^i_{rbc}(t)}{Q^P_{rbc}(t)}, \quad \Phi^i(t) = \frac{Q^i_{blood}(t)}{Q^P_{blood}(t)}, \tag{3}$$

where $i = 1, 2$ denotes the daughter branch 1 and 2 of a generic bifurcation and P denotes the parent branch.

RESULTS AND DISCUSSION

We found that the RBC fluxes $\Psi^i(t)$ and blood flow rates $\Phi^i(t)$ are strongly time-dependent (Figure 2(a)). Even if the time-averaged phase separation is classical (Figure 2(b)) or reverse (Figure 2(c)), the time-dependent phase separation is not constant and it can switch between the two types of partitioning (data are scattered above and below the identity lines in Figure 2(b) and (c)). In agreement with the computational results of Balogh and Bagchi [2], we report that in a complex microchannel network a bifurcation could have a classical partitioning with intermittent episodes of reverse partitioning or vice versa. The origin of these fluctuations may be connected to the temporary difference of the daughter branch resistances due to the passage of individual RBCs.

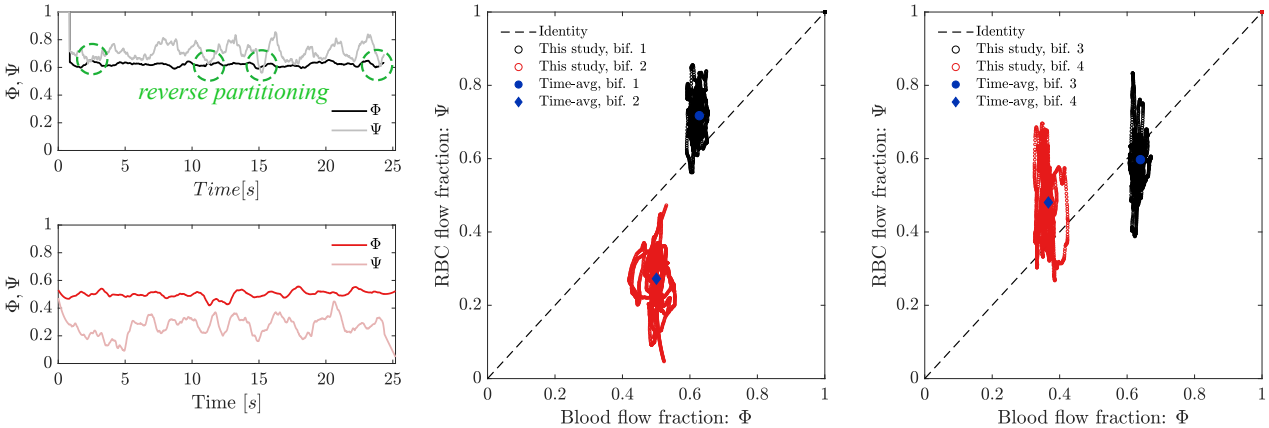

(a) (b) (c)

Figure 2: Time-dependent phase separation (high velocity experiment). (a) Time sequence of $\Phi^i(t)$ (black and red) and $\Psi^i(t)$ (grey and pink) for bifurcations 1 and 2 (cf. Figure 1(a)) exhibiting a time-averaged classical partitioning. (b) $\Phi - \Psi$ diagram for the sequences shown in Figure 2(a). The classical partitioning occurs when $\Psi^i(t) > \Phi^i(t)$ for $\Phi^i(t) > 0.5$ (and vice versa). (c) $\Phi - \Psi$ diagram for bifurcations 3 and 4 (cf. Figure 1(a)) exhibiting a time-averaged reverse partitioning. The reverse partitioning occurs when $\Psi^i(t) < \Phi^i(t)$ for $\Phi^i(t) > 0.5$ (and vice versa). The solid circles indicate the time-averaged results (cf. Figure 1(b)) corresponding to the bifurcations 1,2,3 and 4 indicated in Figure 1(a).

CONCLUSIONS

For the first time we provided *in vitro* quantitative data on the time-averaged and time-dependent RBC partitioning in a complex network and we showed that both time-averaged classical and reverse partitioning contemporary occurred in the network and that selected bifurcations can cycle between the two types of partitioning over time.

References

[1] Mantegazza A., Clavica F., Obrist D. In vitro investigations of red blood cell phase separation in a complex microchannel network. *Biomicrofluidics*. **14**, 014101, 2020. DOI: 10.1063/1.5127840.

[2] Balogh P., Bagchi P. Analysis of red blood cell partitioning at bifurcations in simulated microvascular networks. *Phys. Fluids*. **30**, 5, 2018.

[3] Pries A. R., Secomb T. W., Gaehtgens P., Gross, J. F. Blood flow in microvascular networks. *Circ. Res.*. **67**, 4, 1990.